Astronomy & Astrophysics manuscript no. ms9051 June 30, 2002
(DOI: will be inserted by hand later)

# $H_2O$ and SiO maser emission in Galactic center OH/IR stars*,**

Loránt O. Sjouwerman[1,2,3], Michael Lindqvist[1], Huib Jan van Langevelde[2], and Philip J. Diamond[3,4]

[1] Onsala Space Observatory, S - 439 92 Onsala, Sweden
[2] Joint Institute for VLBI in Europe, Radiosterrenwacht, P.O. Box 2, 7990 AA Dwingeloo, The Netherlands
[3] N.R.A.O. Array Operations Center, P.O. Box 0, Socorro NM 87801, U.S.A.
[4] MERLIN/VLBI National Facility, Jodrell Bank Observatory, Macclesfield, Cheshire SK11 9DL, United Kingdom

Received 20 February 2002; accepted 7 March 2002

**Abstract.** We have performed targeted surveys for 22 GHz $H_2O$ and 43 GHz SiO maser emission in Galactic center OH/IR stars using the Very Large Array. Some of the detections have been used in a previous paper to investigate the possibility of measuring milli-arcsecond accurate positions (to obtain stellar proper motions) in the Galactic center. Here we report on the detection of at least 25 $H_2O$ masers and 18 SiO masers associated with stars within 2° and 15′ of Sgr A*, respectively. This survey has more than doubled the total number of proper motion candidates to at least about 50 stellar objects. The stellar SiO masers are best suited for proper motion studies, although the initial OH, $H_2O$ or SiO maser positions may not be well enough determined to use for a-priori VLBI positions. Serendipitously we also found 8 $H_2O$ masers in the molecular cloud M−0.13−0.08.

**Key words.** Masers – Surveys – Astrometry – Stars: AGB and post-AGB – Galaxy: center

## 1. Introduction

The dynamics of the central ($\sim 50$ pc) region of the Galaxy still poses some interesting questions. The mass distribution, in particular the question whether Sgr A* is a massive black hole, is the most intriguing issue. Outside the immediate $\sim 10$ pc scale environment of Sgr A*, observations provide evidence for a 'bar', and/or a tri-axial bulge. In the past decade many studies to probe the inner Galactic gravitational potential have been performed, using line-of-sight velocities of gas and stars (e.g. Blitz et al. 1993; Genzel et al. 1994; Morris & Serabyn 1996; Mezger et al. 1996). However, in this part of the Galaxy interstellar gas is an unreliable probe to sample the local velocity field, because it might be subject to non-gravitational forces such as stellar winds, radiation pressure and magnetic fields. Also, gas may be transported inward on non-circular motions by a barred potential.

Stellar objects make much better test particles, because they are less susceptible to non-gravitational forces. To improve the present situation, we plan to measure transverse velocities of OH/IR stars in the Galactic center (GC) found by Lindqvist et al. (1992; for further reading on asymptotic giant branch (AGB) and OH/IR stars we recommend Habing 1996 or Iben 1991). All these OH/IR stars observed toward Sgr A* appear to be located in the GC, at an adopted distance of 8 kpc (Reid 1993). But because of severe interstellar scattering toward the GC (Frail et al. 1994; van Langevelde et al. 1992b), the 1612 MHz OH masers are not useful. The higher frequency 22 GHz $H_2O$ and 43 GHz SiO masers, known to reside frequently in OH/IR stars, are more favorable since scattering scales as $\nu^{-2}$. However, so far few surveys for $H_2O$ and SiO masers in the GC have been performed, limiting the number of candidate objects for a proper motion survey. Early targeted single dish observations (Lindqvist et al. 1990, 1991) resulted in 15 high frequency stellar proper motion candidates. More recently additional individual stars with $H_2O$ and SiO masers have become available (e.g. Deguchi et al. 2002; Levine et al. 1995; Menten et al. 1997; Miyazaki et al. 2001), however the number of stellar proper motion candidates was increased by only a handful[1].

We have performed a targeted search for $H_2O$ and SiO maser emission in OH/IR stars in the GC with the Very Large Array (VLA) to obtain a larger sample of proper motion candidates. We describe the observations in Sect.

*Send offprint requests to*: L.O. Sjouwerman (Socorro), e-mail: `lsjouwerm@nrao.edu`

* Figures 1 to 4 are only available in electronic form at http://www.edpsciences.org

** Tables 2, 3, 4 are also available in electronic form at the CDS via anonymous ftp to cdsarc.u-strasbg.fr (130.79.128.5) or via http://cdsweb.u-strasbg.fr/cgi-bin/qcat?J/A+A/

[1] During the final stages of the publication of this paper, Imai et al. (2002 PASJ 54, L19) published a list of 79 43 GHz SiO masers, extending the list presented here considerably.

**Table 1.** Observational summary

| Set | Date | $\nu_{\rm rest}$ GHz | Array | Mode | BW MHz | $\Delta\nu$ kHz | Resolution $'' \times '' \times$km/s | 1733−130 Jy | Sgr A* Jy | RMS $^a$ | Number obs'd | Number det'd |
|---|---|---|---|---|---|---|---|---|---|---|---|---|
| (1) | (2) | (3) | (4) | (5) | (6) | (7) | (8) | (9) | (10) | (11) | (12) | (13) |
| $H_2O$ maser surveys: | | | | | | | | | | | | |
| 1a | 06 Jul 93 | 22.235 | C | 2AC | 6.25 | 97.7 | 2.5×1.9×1.3 | 4.6 | $(0.3)^b$ | 15 | 153 | 21+9 |
| 1b | 08 Jul 93 | | | | | | | 4.0 | 0.7 | | | |
| 1c | 10 Jul 93 | | | | | | | 4.2 | 0.7 | | | |
| 2a | 20 May 94 | 22.235 | $A^1$ | 2BD | 6.25 | 97.7 | 0.3×0.2×1.3 | 6.1 | 0.9 | 10 | 19 | 8+1 |
| 3a | 02 Jun 94 | | $BnA^1$ | | | | | 5.1 | 0.9 | - | 17 | - |
| SiO maser surveys: | | | | | | | | | | | | |
| 2b | 20 May 94 | 42.820 | $A^2$ | 2AC | 12.50 | 390.6 | 1.6×0.7×2.8 | $9^c$ | 1.4 | 60 | 25 | 6 |
| 3b | 02 Jun 94 | | $BnA^2$ | | 6.25 | 97.7 | ×0.7 | $9^c$ | 1.5 | - | 23 | - |
| 4a | 29 Jan 95 | 42.820 | $DnC^3$ | 2AC | 6.25 | 195.3 | 4.3×2.0×1.4 | $9^c$ | 1.1 | 15 | 19 | $15^*$ |
| 4b | | 43.122 | | 2BD | | | | $9^c$ | 1.1 | | | $15^*$ |

1: 17 antennas on the outer stations of the configuration
2: 9 antennas on the inner three stations along each arm
3: 9 antennas with 43 GHz receivers put in a spiral pattern
$a$: Typical RMS noise level in mJy beam$^{-1}$
$b$: On July 8, source J1744−312 instead of Sgr A*
$c$: Adopted 43 GHz flux density for J1733−130
*: A total of 16 sources: 14 sources are detected in both the ($v = 1$) and ($v = 2$) lines; a 15$^{\rm th}$ source in this one line only

2, and the data reduction in Sect. 3. We identify the stellar $H_2O$ and SiO masers, and the $H_2O$ masers associated with star forming regions (SFR's) among our detections in Sect. 4. In Sect. 5, we comment on some aspects of positions and variability. We conclude with the number of proper motion candidates; a first report on measuring their positions with the Very Long Baseline Array (VLBA) can be found in Sjouwerman et al. (1998a). With Sgr A* as phase reference, the new dual-beam Japanese VLBI Exploration of Radio Astrometry (VERA) network (e.g. Hachisuka 2000; Honma et al. 2000) will probably be the preferred instrument to follow up the Sjouwerman et al. (1998a) VLBA efforts with the masers presented in this paper.

The OH names and OH positions used throughout this paper are taken from Lindqvist et al. (1992) unless stated otherwise. Velocities in this paper refer to line-of-sight velocities with respect to the Local Standard of Rest (LSR).

## 2. Observations

In this section we first present the chronology of the observations. The second part of this section contains general comments on the calibration. In 1993, our initial aim was to detect $H_2O$ masers associated with the OH/IR stars with positions accurate enough for follow up VLBI observations; i.e. better than the $1''$ to $2''$ accurate OH positions available. In 1994 we searched for both $H_2O$ and SiO maser emission. During the course of the project, our focus shifted from 22 GHz $H_2O$ masers to 43 GHz SiO masers, because it became clear that SiO masers were a better prospect for obtaining candidates. This is partly because the higher frequency of the SiO maser allows measurements at higher resolution, but moreover because the SiO maser line generally shows less capricious behavior than $H_2O$. Finally, after deciding to use only SiO masers for our proper motion campaign, in 1995 we searched for the ($v = 2$), as well as for the ($v = 1$) line.

### 2.1. Observational history

In July 1993 we used the VLA to search for 22 GHz $H_2O$ masers in the 153 1612 MHz OH masers, most of them associated with OH/IR stars, that were known in the GC at that time[2] from a survey by Lindqvist et al. (1992). The details of these observations, and those of subsequent observations, can be found in the left hand columns of Table 1. Listed are a data set code (1) corresponding to an observing date (2) and rest frequency of the maser line (3), the array configuration (4) and the correlator mode (5), the total bandwidth (6) and channel separation (7).

In 1993 the observing setup was such that phases were calibrated every 15 minutes; the time on-source was 5 minutes. With only a few detections (and an unfortunate calibrator choice), a very low detection rate was obtained. Apart from bad weather, this is possibly also due to the variable nature of the $H_2O$ masers. We concluded that we did not have enough $H_2O$ masers for a proper motion campaign.

In the beginning of 1994, a number of VLA antennas were equipped with 43 GHz receivers, enabling us to search for SiO masers in the OH/IR stars. We selected 48 OH/IR stars from the sample of Lindqvist et al. (1992) which were located within $15'$ of Sgr A*. In May and June 1994 they were observed at 43 GHz in a search for

[2] For a compilation of the data, see the appendix in Sjouwerman et al. (1998b) which also includes more than 50 additional OH/IR stars in the central $35'$ (80 pc) of the GC.

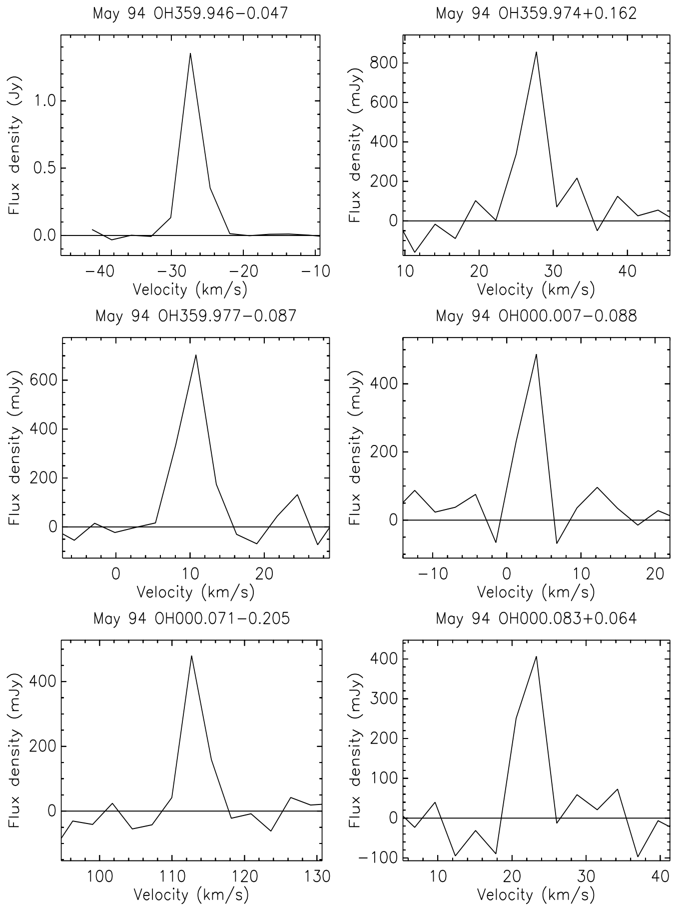


**Fig. 1.** May 1994 spectra of the directly detected 43 GHz SiO ($\mathrm{J} = 1 \rightarrow 0,\ v = 2$) masers. Positions agree with OH positions within $1''$ for all sources

($\mathrm{J} = 1 \rightarrow 0,\ v = 2$) SiO maser emission. At the same time, a similar sample was searched at 22 GHz for $H_2O$ masers as well. The VLA was divided into two sub-arrays: one sub-array with the 43 GHz receivers on the VLA antennas located on the 'inner arms', and another sub-array with the other ('outer arm') antennas observing at 22 GHz.

The phase calibration at 22 GHz was performed every 30 (or 15) minutes with an on-source time of typically 14 minutes. The $H_2O$ maser detection rate was much higher on May 20 ($\approx 50\%$). However, we also encountered broad-band interference hindering us in the bandpass calibration of the June 2 observations; these data were discarded. As this was also the case for the 43 GHz measurements of this day, we presume the interference was generated locally.

For the 43 GHz observations we integrated for 6 minutes on each source and calibrated the phase between source switches. Six sources were detected on May 20 (Fig. 1). Much of the data was lost, however, because of poor phase stability over the relatively long integration time and large array configuration. Phases were stable in several one to three minute intervals, but changed rapidly in between. Visibility averaging or mapping the source did not yield many results. However, with a self-calibration scheme (Sect. 3.2) we found hints that several OH/IR stars indeed had detectable SiO masers. Because of an unreliable bandpass calibration (mentioned in the previous paragraph) in addition to the rapid atmospheric phase fluctuations, the June 2 measurements did not yield any results from direct imaging with, or without bandpass calibration.

In January 1995 we re-observed 19 OH/IR stars, this time searching for SiO maser emission only. The 19 objects were subjectively selected from the observations in 1994 (Sect. 3.2). We observed simultaneously in the 43 GHz ($\mathrm{J} = 1 \rightarrow 0,\ v = 1$) and ($\mathrm{J} = 1 \rightarrow 0,\ v = 2$) transitions. In 1994 we chose only the ($v = 2$) transition of SiO, because it is generally the stronger one in OH/IR stars (Lindqvist et al. 1991; Nyman et al. 1993, 1986). With half the calibration cycle of the 1994 observations and 7 minutes on-source, we obtained a relatively high detection rate (in this subjectively selected sample well over 75%). During these observations the VLA was in its most compact array configuration, with the 43 GHz receivers arranged in a 'spiral configuration' and not on the 'inner' three antennas on each arm as had been the practice before.

### *2.2. Calibrator sources*

On July 7 1993 we used J1744−312 as a phase calibrator, but we noted that it was too weak at 22 GHz. In subsequent observations at 22 as well as at 43 GHz, we chose Sgr A* as phase calibrator (at a J2000 position of $\alpha = 17^{\mathrm{h}}45^{\mathrm{m}}40\overset{\mathrm{s}}{.}0850$, $\delta = -29°00'27\overset{''}{.}790$), despite the extended background radiation of the Sgr A complex. The extended background was mostly resolved out by the array configuration; all baselines longer than 25 and 20 k$\lambda$ are usable for 22 and 43 GHz, respectively.

The first and last observing sequence of 3 targets for each observing day in July 1993 could only be referenced to one calibrator scan, i.e. the visibility phases for these targets had to be extrapolated, possibly introducing some positional inaccuracies. All target sources in the May 1994 and January 1995 observations were enclosed by the phase calibrator Sgr A*, which allowed all visibility phases on the target sources to be interpolated.

For all observations we used J1733−130 for bandpass calibration, which for the 43 GHz observations were preceded by pointing scans on J1733−130 taken every one or two hours. For the 22 GHz observations we included J1331+305 for absolute flux calibration. An accurate flux determination at 43 GHz was complicated by the fact that we used the new VLA 43 GHz receivers before a proper calibration had been done. With an adopted 43 GHz flux for J1733-130 (of 9±3 Jy, VLA test memo #192), we determined fluxes for Sgr A* as shown in column 10 of Table 1. From the fluxes we derive for Sgr A* with this assumption, we expect that the approximate fluxes do not deviate more than 30% from the true values, although we note that Bower et al. (1997) do report an increase in flux for J1733−130 during the interval between the observations. This indicates that our measured fluxes for January 1995 are lower limits. For future reference, we measured a flux of $0.49 \pm 0.03$ Jy for the amplitude calibrator J0137+331 in January 1995 (J1331+305 could not be observed).

## 3. Data reduction

All data sets were calibrated according to a standard spectral line calibration scheme with the NRAO AIPS package. Because of problems determining a bandpass calibration, we quickly scanned the 2 June 1994 22 and 43 GHz data sets for strong masers in the autocorrelation spectra before we had to regard the data as not usable. For all the other data sets, we made image cubes of about 25″ in diameter around the OH maser positions. In cases where we pointed the telescopes such that more than one OH/IR star would fall in the primary beam (and velocity coverage), we chose to image the full primary beam (2′ or 1′ for 22 and 43 GHz respectively) which is less troublesome than to image each position separately. For these larger image cubes, we searched the OH/IR star positions and also detected several $H_2O$ masers serendipitously. Below we will only pay some attention to our serendipitous detections of OH359.956−0.050, and the $H_2O$ masers in the molecular cloud M−0.13−0.08. A summary of the image cubes can be found in Table 1, where we give the spatial and spectral resolution of the image cubes (8), the measured fluxes for our calibrators (9), (10), a representative value for the noise in the image cube (11), the total number of fields searched for emission (12) and the number of detections in OH/IR stars + tentative associations with OH/IR stars in those fields (13).

### 3.1. $H_2O$ maser profiles

Many studies of $H_2O$ masers in different types of objects have been performed in collections of late-type stars with circumstellar environments originating from mass-loss of the central object: a mixture of supergiants, semi-regular variable stars, Mira and OH/IR stars (Engels et al. 1986, 1988; Nyman et al. 1993, 1986; Olnon et al. 1980 and Engels & Lewis 1996; see also the compilation of other objects in Brand et al. 1994; Comoretto et al. 1990). From these studies, a distinction between the different types of stars, and star forming regions, may be made based on the characteristics of the $H_2O$ and OH maser emission. However, the classification scheme is valid in a statistical sense, and thus not watertight, in particular in the GC where helpful additional optical or infrared information is difficult to obtain.

For OH/IR stars, Engels et al. (1986) divided the $H_2O$ maser detections into two types, A and B, characterized by their spectral shape. Olnon et al. (1980) have proposed a similar sub-division using several OH maser lines for different types of late-type variable stars. Type A masers show a single $H_2O$ maser peak close to the systemic velocity; type B $H_2O$ masers are double peaked and usually symmetric around the mean, systemic velocity. Most of the type B $H_2O$ maser have a smaller velocity separation between the $H_2O$ maser peaks than the 1612 MHz OH maser, although occasionally the $H_2O$ maser separation is a few km $s^{-1}$ larger compared to OH. Whether a source shows an A or B (or A/B, Engels & Lewis 1996) type $H_2O$ maser is strongly dependent on the IRAS colors of the source; blue Miras predominantly show type A, red OH/IR stars mainly type B spectra (Engels & Lewis 1996). The variability of the maser is reflected in the peak flux density of the emission at fixed velocities; not in changing velocity profiles (with a reservation for rare sources that show mode switching; Engels et al. 1997). In our search for detections we were helped by these characterizations and the knowledge of the 1612 MHz OH profiles. Most of our $H_2O$ maser detections toward the OH maser sources can be characterized as type A or type B $H_2O$ masers. Because of sensitivity limits, we often find only one (the dominant) peak of a B-type double peaked $H_2O$ maser profile, and also in our sample the blue shifted peak is in a statistical sense more dominant than the red shifted one (see discussion in Engels & Lewis 1996). Supergiants, OB star associations and star forming regions are known to have much more complex, and changing $H_2O$ (and OH) maser spectral profiles (e.g. Engels & Lewis 1996; Engels et al. 1988; Genzel & Downes 1977, 1979; Reid et al. 1988). Probably typical examples of such SFR's in this survey are sources OH359.751−0.371 and OH359.936−0.144.

### 3.2. SiO maser profiles; self-calibration

Inspection of the 43 GHz image cubes of the 20 May 1994 observations yielded 6 clear SiO maser detections out of 25 within the positional accuracy (1″) and at about the stellar velocity derived from the OH maser (Fig. 1). From Lindqvist et al. (1992) and Sjouwerman et al. (1998b) we have OH positions accurate to $\sim 1''$. Here we used the positions from Lindqvist et al. (1992) because the survey was done before the Sjouwerman et al. (1998b) survey was finalized; see also Sect. 5.1. However, some tentative and weak SiO masers deviate considerably (up to 10″) from these OH positions. We think these positional differences are due to phase calibration problems. In many of the image cubes we found channels with emission exceeding the noise. We believe that the emission is real since we had problems with the phase calibration. Analyzing the data of the reliable detections, we could see that the visibility phases were stable over several one minute scans, but could switch more than a radian in the next minute. Using knowledge on the spectral profile of SiO masers, we attempted to image more sources, or at least to obtain candidates for re-observation. In doing this we made use of the fact that SiO emission is found around the stellar velocity (the mean of the OH maser peaks) and usually has a width of about 5 km $s^{-1}$, in our data thus a few channels wide (e.g. Lindqvist et al. 1991; Nyman et al. 1986). Furthermore, we assume the noise in individual, uniformly weighted frequency channels to be mostly inde-

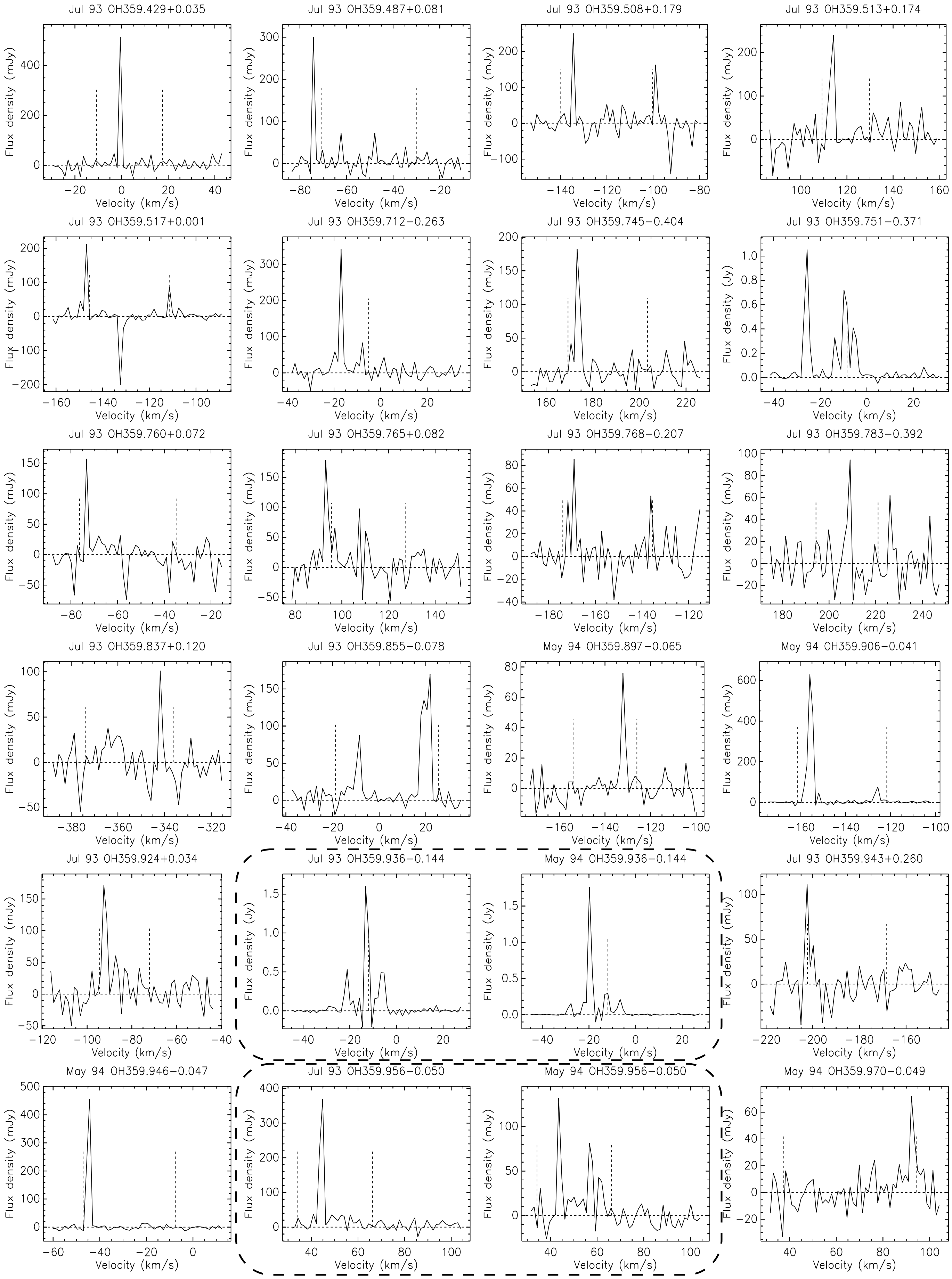


**Fig. 2.** Spectra of the 22 GHz $H_2O$ maser detections in July 1993 and May 1994. The velocity resolution is 1.3 km $s^{-1}$, and the two boxed spectra each are spectra of the same source, OH359.936−0.144 and OH359.956−0.050, in July 1993 and May 1994

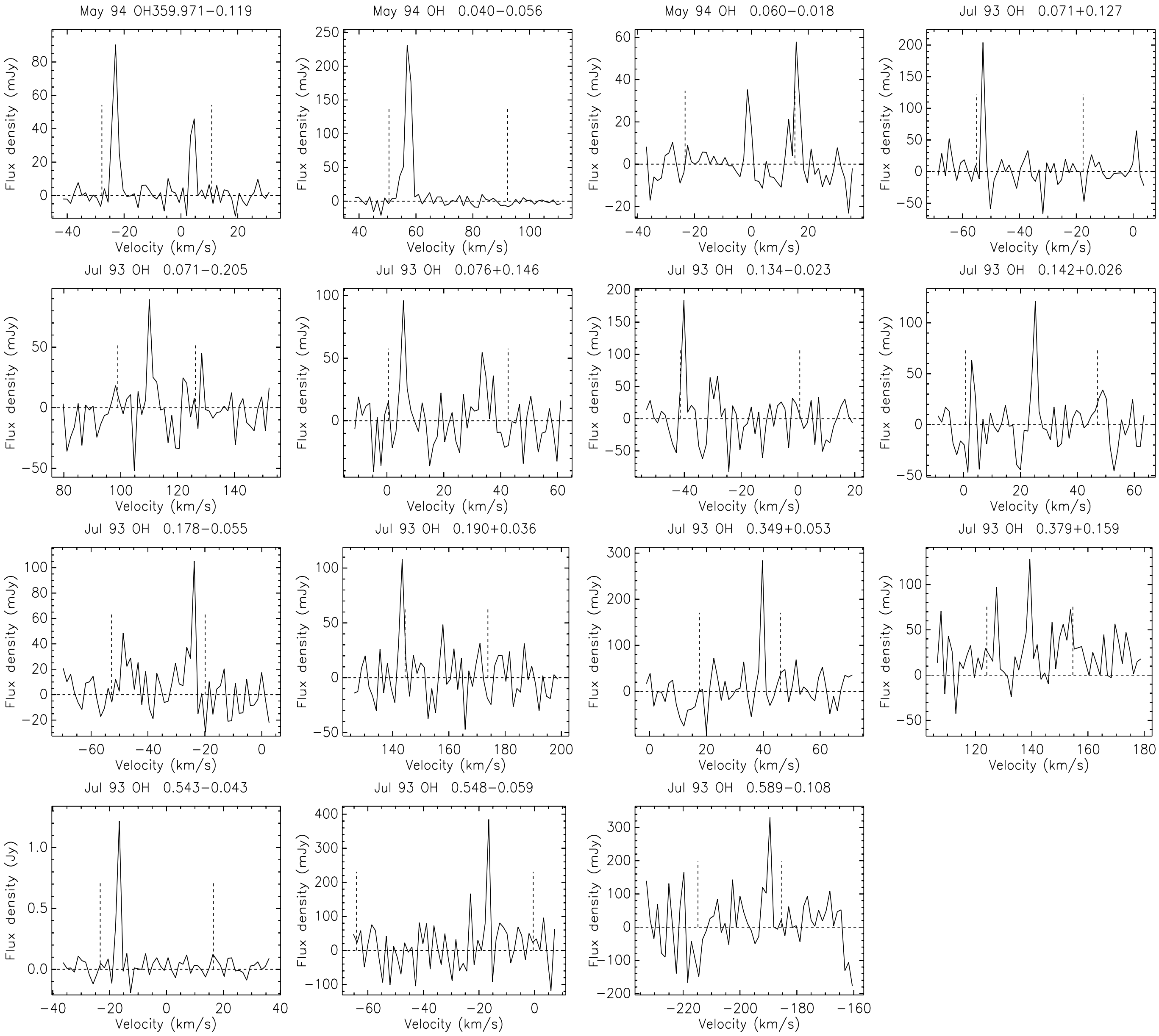


**Fig. 2.** Spectra of the 22 GHz $H_2O$ maser detections in July 1993 and May 1994 (continued)

pendent and take the interval of atmospheric phase stability to be one minute.

Assuming that a certain channel covers a part of the broad SiO maser profile, we self-calibrated the data from this channel assuming a point source model. The self-calibration solution was then applied to all channels. Now, if the channel does not contain line emission, noise in this channel will add up into a spurious detection. However, because the noise in each channel is independent, the solution for this channel applied to the next channels will not yield a similar addition of noise there, thereby yielding no significant systematic emission at this location in the adjacent channels.

However, we found many sources – also in the 'unusable' 43 GHz June 1994 observations – for which a solution for one frequency channel aligned flux in several consecutive channels. We regarded such sources as worthy of further investigation and their names were collected for the re-observation program. Because of the extra contribution of the noise in one channel and a missing bandpass calibration for the June 2 data set, spectral profiles and fluxes are not determined for these sources. A chance alignment of another source with the same line-of-sight velocity in the primary beam, other than the source we pointed at, seems unlikely but cannot be excluded. However, the justification of the method is shown by the successful detection of almost all of these re-observed sources in January 1995. For the $H_2O$ masers, the spectral profile is much less regular and many maser spots are spectrally unresolved in our data sets. Hence, the scheme outlined above unfortunately does not work properly for the $H_2O$ masers.

**Table 2.** $H_2O$ maser detections in targeted 1612 MHz OH masers in the Galactic center

| OH Name | Set | $H_2O$ Position (J2000) R.A. | Dec. | $\Delta$ $''$ | Range $V_{OH}$ km/s | | $V_{blue}$ | km/s | $V_{red}$ | $S_{peak}$ Jy | $I_{total}$ [a] |
|---|---|---|---|---|---|---|---|---|---|---|---|
| (1) | (2) | (3) | (4) | (5) | (6) | (7) | (8) | (9) | (10) | (11) | (12) |
| 359.429+0.035* | 1a | 17 44 7.372 | −29 24 7.65 | 10.72 | −10.8 | 17.6 | −0.6 | | | 0.50 | 0.74 |
| 359.487+0.081* | 1a | 17 44 4.098 | −29 19 54.90 | 7.74 | −70.9 | −30.1 | −74.2 | −47.9 | | 0.30 | 0.59 |
| 359.508+0.179* | 1b | 17 43 45.624 | −29 15 34.86 | 14.58 | −139.9 | −100.2 | −134.5 | | −98.9 | 0.25 | 0.56 |
| 359.513+0.174 | 1c | 17 43 46.772 | −29 15 37.83 | 1.02 | 109.2 | 129.7 | 114.2 | | | 0.23 | 0.95 |
| 359.517+0.001 | 1a | 17 44 27.655 | −29 20 48.63 | 2.33 | −145.6 | −111.5 | −146.9 | | −111.4 | 0.22 | 0.44 |
| 359.712−0.263 | 1c | 17 45 57.566 | −29 19 9.81 | 0.17 | | −5.1 | | −17.0 | −7.7 | 0.35 | 1.08 |
| 359.745−0.404 | 1b | 17 46 35.629 | −29 21 49.68 | 2.28 | 169.4 | 203.5 | 173.3 | | | 0.18 | 0.56 |
| 359.751−0.371† | 1b | 17 46 28.712 | −29 20 29.16 | 1.36 | | −8.5 | −25.6 | | −9.8 | 1.05 | 7.95 |
| 359.760+0.072 | 1c | 17 44 45.989 | −29 6 13.86 | 0.59 | −76.3 | −34.6 | −73.3 | | | 0.14 | 0.75 |
| 359.765+0.082 | 1c | 17 44 44.517 | −29 5 40.17 | 3.11 | 95.6 | 127.4 | 93.1 | 107.6 | | 0.17 | 1.69 |
| 359.768−0.207 | 1a | 17 45 52.676 | −29 14 33.29 | 2.57 | −173.9 | −135.4 | −169.1 | | −136.2 | 0.08 | 0.28 |
| 359.783−0.392 | 1a | 17 46 38.348 | −29 19 24.66 | 6.97 | 194.4 | 221.0 | | 209.0 | 226.1 | 0.10 | 0.12 |
| 359.837+0.120 | 1a | 17 44 45.842 | −29 0 42.59 | 2.49 | −374 | −336 | | −341.8 | | 0.09 | 0.39 |
| 359.855−0.078 | 1a | 17 45 34.734 | −29 6 2.70 | 1.01 | −18.7 | 25.5 | −8.4 | | 21.8 | 0.16 | 2.03 |
| 359.897−0.065 | 2a | 17 45 38.396 | −29 3 35.83 | 5.92 | −154 | −126 | | −132.1 | | 0.08 | 0.15 |
| 359.906−0.041 | 2a | 17 45 33.528 | −29 2 16.24 | 0.51 | −161.4 | −121.7 | −156.0 | | −125.7 | 0.63 | 1.96 |
| 359.924+0.034* | 1c | 17 45 18.961 | −28 58 56.94 | 5.61 | −94.5 | −72.1 | −92.5 | | | 0.17 | 0.53 |
| 359.936−0.144† | 1b | 17 46 1.966 | −29 3 58.78 | 1.32 | | −11.9 | | −13.2 | | 1.52 | 9.47 |
| ,, | 2a | 1.969 | 58.48 | 1.00 | | ,, | | −19.8 | | 1.88 | 5.76 |
| 359.943+0.260 | 1a | 17 44 28.035 | −28 50 49.08 | 7.54 | −202.3 | −168.3 | −202.4 | | | 0.10 | 0.44 |
| 359.946−0.047 | 2a | 17 45 40.674 | −29 0 23.51 | 0.74 | −47.1 | −7.4 | −44.3 | | | 0.46 | 0.93 |
| 359.956−0.050 | 1c | 17 45 42.749 | −28 59 56.83 | 1.31 | 34.2 | 66.2 | 44.8 | | | 0.35 | 1.44 |
| ,, | 2a | 42.763 | 57.20 | 1.24 | ,, | ,, | 43.5 | | 56.7 | 0.16 | 0.62 |
| 359.970−0.049 | 2a | 17 45 44.356 | −28 59 12.99 | 0.26 | 37.5 | 94.5 | | | 92.2 | 0.07 | 0.31 |
| 359.971−0.119 | 2a | 17 46 0.990 | −29 1 23.04 | 0.57 | −27.8 | 10.8 | −23.0 | | 4.7 | 0.09 | 0.35 |
| 0.040−0.056 | 2a | 17 45 56.127 | −28 55 51.71 | 0.47 | 50.5 | 92.2 | 56.9 | | | 0.24 | 0.77 |
| 0.060−0.018* | 2a | 17 45 49.244 | −28 53 29.43 | 12.93 | −23.3 | 15.3 | | −1.4 | 15.7 | 0.06 | 0.12 |
| 0.071+0.127 | 1c | 17 45 17.635 | −28 48 36.46 | 1.00 | −55.0 | −17.6 | −52.8 | | | 0.20 | 0.36 |
| 0.071−0.205 | 1a | 17 46 35.720 | −28 58 58.39 | 5.15 | 99.0 | 126.3 | | 110.1 | 128.5 | 0.10 | 0.10 |
| 0.076+0.146 | 1b | 17 45 13.876 | −28 47 42.05 | 1.77 | 0.6 | 42.6 | 5.8 | | 33.5 | 0.09 | 0.63 |
| 0.134−0.023* | 1c | 17 46 1.417 | −28 50 6.57 | 6.31 | −41.4 | 0.6 | −40.2 | | | 0.18 | 0.60 |
| 0.142+0.026* | 1b | 17 45 52.255 | −28 48 14.11 | 13.71 | 0.6 | 47.1 | 2.8 | 25.2 | 48.9 | 0.12 | 0.32 |
| 0.178−0.055* | 1a | 17 46 15.825 | −28 48 35.62 | 13.61 | −52.8 | −19.9 | −48.8 | | −23.7 | 0.11 | 0.46 |
| 0.190+0.036* | 1a | 17 45 55.315 | −28 45 27.21 | 10.72 | 144.4 | 173.9 | 143.4 | | | 0.11 | 0.19 |
| 0.349+0.053* | 1c | 17 46 14.959 | −28 36 46.92 | 9.08 | 17.6 | 46.0 | | 39.7 | | 0.29 | 0.47 |
| 0.379+0.159 | 1a | 17 45 54.059 | −28 31 45.20 | 3.54 | 124.0 | 154.6 | 127.4 | 139.3 | 153.8 | 0.12 | 0.24 |
| 0.543−0.043 | 1b | 17 47 4.897 | −28 29 39.78 | 4.29 | −23.3 | 16.5 | −16.6 | | | 1.20 | 5.41 |
| 0.548−0.059 | 1c | 17 47 9.076 | −28 29 51.65 | 4.75 | −64.1 | −0.5 | | | −16.5 | 0.40 | 0.63 |
| 0.589−0.108 | 1c | 17 47 25.633 | −28 29 20.65 | 7.89 | −214.8 | −185.3 | | −202.6 | −189.5 | 0.32 | 0.87 |

*: tentative association; see discussion in Sect. 3 and 4 [a]: units in Jy km/s
†: SFR, not stellar (OH/IR); see discussion in Sect. 4.1

## 4. Results

In summary we have 25 $H_2O$ maser detections in OH/IR stars, 2 $H_2O$ maser detections in SFR's, and 10 $H_2O$ masers tentatively associated with OH/IR stars (see below). We have also detected 18 SiO masers in OH/IR stars. The $H_2O$ maser detections associated with the OH sources are given in Table 2 and Fig. 2, $H_2O$ masers associated with the molecular cloud M−0.13−0.08 in Table 3 and Fig. 3, and the SiO maser detections in OH/IR stars in Table 4 and Figs. 1 and 4. The clear non-detections and non-redetections are summarized in Table 5.

All detections, in Tables 2, 3 and 4, have entries for the name of the source in Galactic coordinates (1), the code of the data set (2) and the position in J2000 coordinates (3), (4), with either the offset ($\Delta$) from the original OH position (5), (Tables 2 and 4), or the maximum of the formal error in either R.A. or Dec. in arcseconds ($\epsilon$) as measured with the AIPS task IMFIT (5), (Table 3). In Table 2 we added the velocity range of the OH maser (6),

**Table 3.** Serendipitous $H_2O$ maser detections in M−0.13−0.08

| $H_2O$ Name | Set | Position (J2000) R.A. | Dec. | $\epsilon$ ″ | $V_{blue}$ | $V_{central}$ km/s | $V_{red}$ | $S_{peak}$ Jy | $I_{total}$ Jy km/s | Note |
|---|---|---|---|---|---|---|---|---|---|---|
| (1) | (2) | (3) | (4) | (5) | (8) | (9) | (10) | (11) | (12) | |
| 359.859−0.079 | 2a | 17 45 35.461 | −29 5 47.86 | 0.021 | | 12.6 | | 0.28 | 0.48 | |
| 359.861−0.082 | 1a | 17 45 36.297 | −29 5 49.63 | 0.077 | | 8.7 | | 0.25 | 1.85 | |
| 861−0.082 | 2a | 36.377 | 49.16 | 0.028 | | 10.0 | | 0.31 | 1.80 | |
| 359.864−0.084 | 1a | 17 45 37.458 | −29 5 44.28 | 0.093 | 4.7 | | 11.3 | 0.14 | 0.77 | |
| 359.864−0.083 | 2a | 17 45 37.214 | −29 5 41.48 | 0.040 | | 10.0 | | 0.13 | 0.33 | |
| 359.864−0.084 | 1a | 17 45 37.527 | −29 5 42.83 | 0.124 | | 3.4 | | 0.12 | 1.48 | |
| 359.864−0.085 | 2a | 17 45 37.676 | −29 5 43.80 | 0.015 | | 28.4 | | 0.41 | 0.87 | Star? Sect. 4.1 |
| 359.865−0.085 | 1a | 17 45 37.832 | −29 5 42.88 | 0.062 | −17.7 | | −8.4 | 0.95 | 6.91 | |
| 865−0.085 | 2a | 37.917 | 42.64 | 0.019 | −13.7 | | −7.1 | 0.29 | 1.22 | |
| 359.874−0.079 | 1a | 17 45 37.754 | −29 5 2.99 | 0.043 | | −13.7 | | 0.15 | 0.98 | |

**Table 4.** SiO maser detections in OH/IR stars in the Galactic center

| OH Name | Set | SiO Position (J2000) R.A. | Dec. | Δ ″ | ($v=2$), 42.820 GHz $V_{system}$ km/s | $S_{peak}$ Jy | $I_{total}$ Jy km/s | ($v=1$), 43.122 GHz $V_{system}$ km/s | $S_{peak}$ Jy | $I_{total}$ Jy km/s |
|---|---|---|---|---|---|---|---|---|---|---|
| (1) | (2) | (3) | (4) | (5) | (6) | (7) | (8) | (9) | (10) | (11) |
| 359.763−0.042 | 4b | 17 45 13.069 | −29 9 34.99 | 1.04 | 122.7 | 0.17 | 0.25 | 122.7 | 0.19 | 0.61 |
| 359.765+0.082 | 4b | 17 44 44.460 | −29 5 37.33 | 0.37 | 111.5 | 0.62 | 2.87 | 111.5 | 0.97 | 4.05 |
| 359.778+0.010 | 4a | 17 45 3.244 | −29 7 12.35 | 0.29 | −28.4 | 0.50 | 1.47 | −28.4 | 0.58 | 1.47 |
| 359.803−0.021 | 4a | 17 45 13.928 | −29 6 55.17 | 1.91 | −16.3 | 0.75 | 3.79 | −15.0 | 0.31 | 1.84 |
| 359.810−0.070 | 4a | 17 45 26.401 | −29 8 2.30 | 1.96 | −36.6 | 0.29 | 1.58 | −33.9 | 0.22 | 1.11 |
| 359.855−0.078 | 4b | 17 45 34.769 | −29 6 3.14 | 1.01 | 4.0 | 0.41 | 2.62 | 4.0 | 0.38 | 1.76 |
| 359.946−0.047 | 4b | 17 45 40.639 | −29 0 24.10 | 0.22 | −27.3 | 0.37 | 3.47 | −27.3 | 0.44 | 2.96 |
| 359.952−0.036 | 4a | 17 45 38.676 | −28 59 45.57 | 0.55 | 84.9 | 0.19 | 0.27 | 84.9 | 0.28 | 1.21 |
| 359.954−0.041 | 4a | 17 45 40.250 | −28 59 46.86 | 1.37 | 69.9 | 0.29 | 1.33 | 71.3 | 0.19 | 1.64 |
| 359.971−0.119 | 4a | 17 46 0.967 | −29 1 22.77 | 0.51 | −8.5 | 2.13 | 9.87 | −9.9 | 0.47 | 1.72 |
| 359.974+0.162 | 4a | 17 44 55.639 | −28 52 26.21 | 0.77 | 27.7 | 0.57 | 2.24 | 27.7 | 0.51 | 3.38 |
| 359.977−0.087 | 2b | 17 45 54.368 | −29 0 2.66 | 0.17 | 10.8* | 0.70* | 3.80* | not detected in Jan. 95 | | |
| 359.996−0.144 | 4b | 17 46 10.413 | −29 0 51.17 | 2.41 | - | - | - | −32.3 | 0.34 | 0.79 |
| 0.007−0.088 | 2b | 17 45 58.956 | −28 58 34.83 | 0.40 | 4.0* | 0.43* | 1.52* | not detected in Jan. 95 | | |
| 0.071−0.205 | 4a | 17 46 35.364 | −28 58 56.92 | 0.68 | 114.1 | 0.55 | 1.20 | 114.1 | 0.46 | 1.00 |
| 0.079−0.114 | 4a | 17 46 15.377 | −28 55 42.52 | 1.35 | 51.4 | 0.21 | 2.48 | - | - | - |
| 0.083+0.064 | 4a | 17 45 34.270 | −28 49 55.93 | 1.45 | 23.3 | 0.27 | 0.92 | 23.3 | 0.28 | 1.17 |
| 0.142+0.026 | 4a | 17 45 51.339 | −28 48 6.96 | 0.11 | 23.9 | 0.26 | 1.21 | 23.9 | 0.27 | 0.77 |

*: measurement of May 1994 (Fig. 1), not detected in either 43 GHz SiO line in Jan 1995 (Fig. 4)

(7), for comparison with the $H_2O$ maser velocities. The OH maser velocity range is also indicated in the spectra in Fig. 2 by vertical dashed lines. Furthermore, for the $H_2O$ masers in Tables 2 and 3, we list the velocity of the associated most blue shifted (8), the central (9), and the most red shifted (10) components (where appropriate), the highest peak flux of the profile (11), and the total (spatially and spectrally) integrated line flux (12). An asterisk after the OH name for the $H_2O$ maser in Table 2 indicates whether the measurements concern tentative associations. Table 4 is completed by listing the mean velocity (6), (9), the highest peak flux (7), (10), and the total integrated line flux (8), (11) for the ($v=2$), and for the ($v=1$) transition respectively. We chose the position with the smallest formal error; ($v=2$) if 'Set' in column 2 lists '2b' or '4a', ($v=1$) for 'Set' equal to '4b'; they are however consistent with each other to the sub-arcsecond level. The spectra for all detections can be found in Figs. 1, 2, 3 and 4.

As the initial OH positions have an accuracy of 1-2″ (Habing et al. 1983; Lindqvist et al. 1992; Sjouwerman & van Langevelde 1996; van Langevelde et al. 1992a), an $H_2O$ or SiO maser with the 'proper' velocity signature (Sect. 3) within this error is considered to be clearly associated with the OH maser. This is the case for 14 $H_2O$ maser sources, and for almost all 18 SiO maser sources.

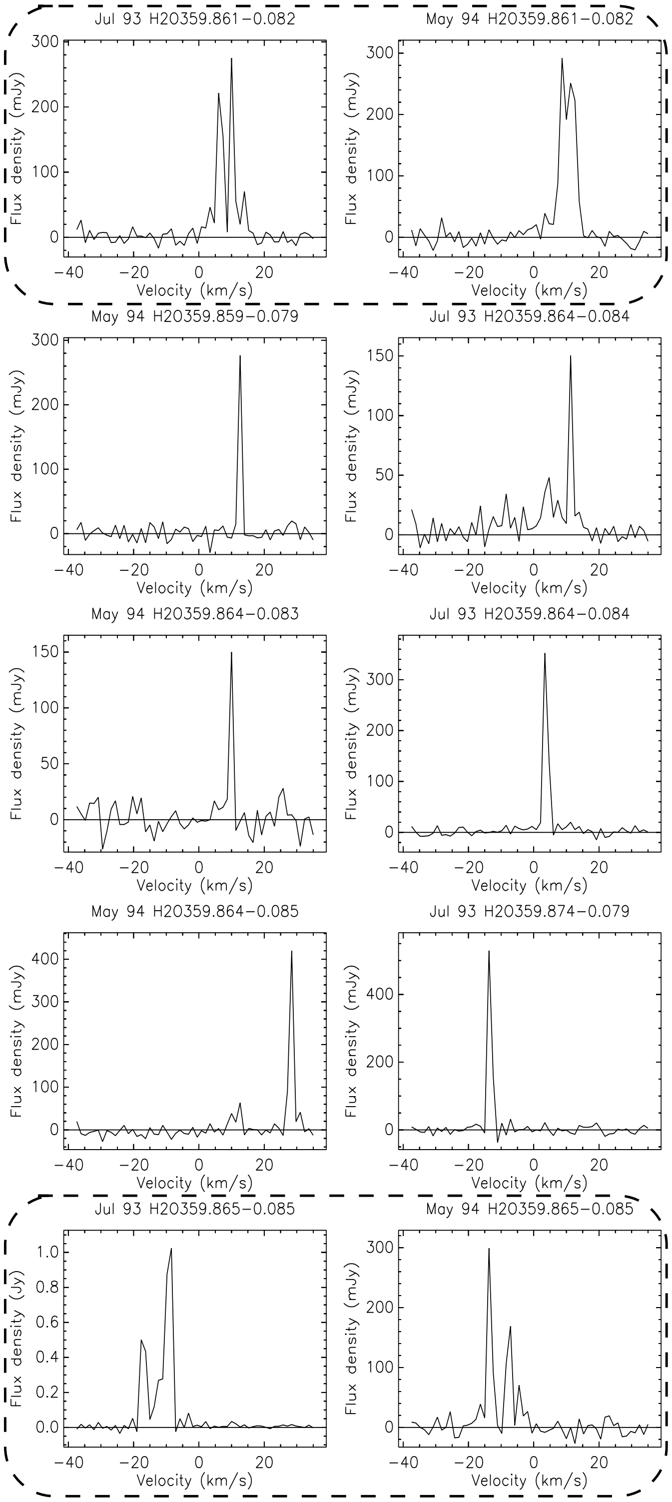


**Fig. 3.** $H_2O$ masers in M−0.13−0.08. The two boxed spectra are two spectra of the same source, OH359.861−0.082 and OH359.865−0.085, in July 1993 and May 1994

For the 22 GHz July 1993 observations that are not well calibrated, we allowed an additional 8 sources with a positional difference of twice the synthesized beam size (i.e. an offset of 5″ for July 1993); it might also be possible that the initial position accuracy is actually a bit worse than the claimed 1 to 2″. Larger deviations, up to ∼ 3 synthesized beams (8″) in July 1993, have been accepted as a detection of an $H_2O$ maser in the OH/IR star for 5 sources with a very high systemic stellar velocity ($|V| > 100$ km $s^{-1}$). Although we are observing toward the central parsecs of the Galaxy, toward a steep gravitational potential, it seems unlikely that strong $H_2O$ masers could form in SFR's at these velocities, and in particular at the same time coincide within the position and velocity range of the old, supposedly dynamically relaxed OH/IR star. Finally, another 10 tentative associations are included for which we suggest that the $H_2O$ maser is associated with the OH/IR star. Although they lack sufficient positional coincidence for a definite association, the velocity signature resembles the expected behavior for OH/IR stars enough to be included in the results. Their positional offset from the OH position ranges from 5.″6 to 14.″6. These and other individual associations are commented on in Sect. 4.1.

Using this scheme, we detected 30 (21 + 9 tentative) $H_2O$ maser sources associated with OH masers, and serendipitously 5 $H_2O$ masers in the molecular cloud M−0.13−0.08 in July 1993. In May 1994 we detected 9 $H_2O$ maser sources (8 + 1 tentative association). Among the 5 $H_2O$ masers that we found serendipitously in M−0.13−0.08 in May 1994, 2 of the $H_2O$ masers were also detected in July 1993. We attribute the newly appeared masers between July 1993 and May 1994 in this cloud due to maser variability, which is common in SFR's. Source OH359.956−0.050 (e.g. Sjouwerman & van Langevelde 1996) was serendipitously found as an $H_2O$ maser in both the July 1993 as well as in the May 1994 data. It is an OH/IR star and therefore included in the survey. We discarded all other (possible) detections in the $H_2O$ maser line that we could not associate with either a position or velocity of the targeted OH maser. We did the same to the $H_2O$ masers that were clearly associated with the OH masers in the SFR in Sgr B2.

For the 22 GHz May 1994 and 43 GHz January 1995 observations, we also give the non-detections in Table 5 in cases where we can firmly conclude this. We do not give the non-detections for the July 1993 (over 100 sources) and June 1994 22 GHz observations, and also not for the May and June 1994 43 GHz observations, because many might have been detected if it had been possible to improve the calibration. Positions and spectra measured for many (tentative) associations in these data sets may have very large offsets (on the order of 10″) or improper channel alignment which made clear (spectral) identification difficult. Looking at the data, we suspect that there are a number of $H_2O$ masers (either in OH/IR stars or SFR's) to be found in several of our observed fields, but we lack sufficient sensitivity or calibration to make a definite statement about this. An exception is the field around M−0.13−0.08 as noted above. See also Menten et al. (1997) for additional $H_2O$ masers around Sgr A*, and Sjouwerman et al. (1998b) for newly found OH/IR stars that can be searched for $H_2O$ and SiO masers (Sjouwerman et al., *in preparation*).

For an impression of the long term variability and the occurrence of multiple maser lines, we list the sources that were detected (denoted with '+') in both our, or other, surveys in Table 6. However, the overlap of the (reliable part of the) data sets is generally small and non-detections, or non-redetections, (denoted with '−') might be due to low sensitivity or variability. Some of the multiple detected sources could provide an opportunity to measure a proper motion of an individual star in the $H_2O$ and SiO maser lines independently.

### *4.1. Notes on individual $H_2O$ masers*

We now compare our detections with the 1612 MHz OH maser detections from our input catalog. In particular, we comment on all tentative associations (Sect. 3.1.), and the possible nature of the objects ("SFR" or "OH/IR") that are not obviously OH/IR stars. The non-detections from Lindqvist et al. (1990) in their $H_2O$ survey in a subset of this survey may largely be due, in combination with maser variability, to low sensitivity – their RMS is typically 100 to 130 mJy, about a factor of 10 higher than this work.

**OH359.429+0.035:** Tentative association and extrapolated visibility phases. In the 1612 MHz OH maser line, this source has a peculiar OH spectrum from which Lindqvist et al. (1992) could not clearly conclude whether this star is an OH/IR star or connected to a star forming region. With the detection of $H_2O$ maser emission close to the (proposed) stellar velocity, which notably lines up in velocity with the extra central OH peak, we conclude it is most probably a type A $H_2O$ maser of an OH/IR star or a post-AGB star.

**OH359.487+0.081:** Extrapolated visibility phases, which makes the position registration unclear. It is detected three beams away from the OH position, but we conclude it to be a real association, labeled tentative for consistency.

**OH359.508+0.179:** Tentative association and extrapolated visibility phases. Although the $H_2O$ emission is nearly 15″ offset from the OH emission, we do observe 2 $H_2O$ maser peaks in the same line-of-sight with velocities close to the velocity of the two OH peaks, making it, at this high velocity, likely to originate from the same (stellar) source.

**OH359.513+0.174:** Extrapolated visibility phases and within the position to be associated with the OH maser.

**OH359.517+0.001:** Extrapolated visibility phases. Coincident with the OH position and the OH maser velocities. The nature of the absorption profile is unclear.

**OH359.712−0.263:** Detected as a single 1612 MHz OH peak at a velocity of $-5$ km s$^{-1}$, but shows the expected $H_2O$ maser profile of an OH/IR star of type A (or A/B) with the systemic velocity close to $-17$ km s$^{-1}$.

**OH359.751−0.371:** Also a single peak 1612 MHz OH detection at $-8.5$ km s$^{-1}$. The $H_2O$ maser line spectrum resembles spectra of young stellar objects with CO outflows in SFR's (e.g. Felli et al. 1992; Genzel & Downes 1977). However, the source does not show up in the search for compact radio continuum sources (H II regions) by Downes et al. (1979), possibly because it is just outside their surveyed area. Levine et al. (unpublished, E. Schulman, pers. comm.) find $H_2O$ emission at velocities from $-82.1$ to $-66.3$ km s$^{-1}$ at this position, supporting the identification with a SFR in this direction.

**OH359.783−0.392:** Association based on the high velocity of the maser.

**OH359.837+0.120:** OH name and OH position taken from van Langevelde et al. (1992a). A high velocity OH/IR star ($|V_{\rm LSR}| > 250$ km s$^{-1}$), which also has been confirmed in the 1612 MHz OH line in Sjouwerman et al. (1998b).

**All sources around $\mathbf{H_2O359.86-0.08}$:** (Table 3, Fig. 3) In this region one finds the dense molecular cloud core M−0.13−0.08, an ultra compact H II region, and two[3] OH/IR stars. By fitting both OH/IR stars in one beam we happened to point at one of the dense cores of M−0.13−0.08. One of these OH/IR stars (OH359.855−0.078) is detected as an $H_2O$ maser, and with the possible exception of $H_2O$359.864−0.085 (see next note), all the other $H_2O$ masers found here are likely to be connected to the formation of stars. At least two of these masers had been found previously by Okumura et al. (1989) and in single beam observations by Guesten & Downes (1983) and Lindqvist et al. (1990; note the resemblance with the spectra of Guesten & Downes 1983, and our weak source $H_2O$359.864−0.084 from our July 1993 observations; it is not to be confused with the strong source $H_2O$359.865−0.085 in our list). For easy comparison, we show these spectra in Fig. 3 separate from the spectra in Fig. 2. We defer a proper discussion of these detections – together with new observations – in this star forming region to a forthcoming paper.

**$\mathbf{H_2O359.864-0.085}$:** A possible characteristic double peaked point-like $H_2O$ maser (Table 3; displayed in Fig. 3) which has not been detected in the 1612 MHz OH line by either Lindqvist et al. (1992) or Sjouwerman et al. (1998b). Therefore, we hesitate to classify this object to be an OH/IR star. We cannot exclude that the $H_2O$ emission at 13 km s$^{-1}$ is a side-lobe of $H_2O$359.861−0.082 in which case this detection would be one of the many SFR's in the direction of M−0.13−0.08. We are more comfortable with a classification as SFR.

**OH359.897−0.065:** OH name and OH position taken from te Te Lintel Hekkert et al. (1989), who quoted OH359.90−0.07 in Habing et al. (1983). Our $H_2O$ position is 6″ off, whereas all our other May 1994 (high resolution A configuration) detections are within about 1″. It is possi-

[3] Actually there are three OH/IR stars in this field: OH359.855−0.078, OH359.880−0.087, and OH359.875−0.091. The latter was found in the OH maser line after this survey by Sjouwerman et al. (1998b) with a line-of-sight velocity within the here surveyed region. It is however not detected in the $H_2O$ maser line here, nor in the follow up observations in July 1999 (Sjouwerman et al., *in preparation*). Its $H_2O$ maser might however been accidentally observed by Lindqvist et al. (1990) as $H_2O$359.89−0.07, consistent with the OH maser velocity.

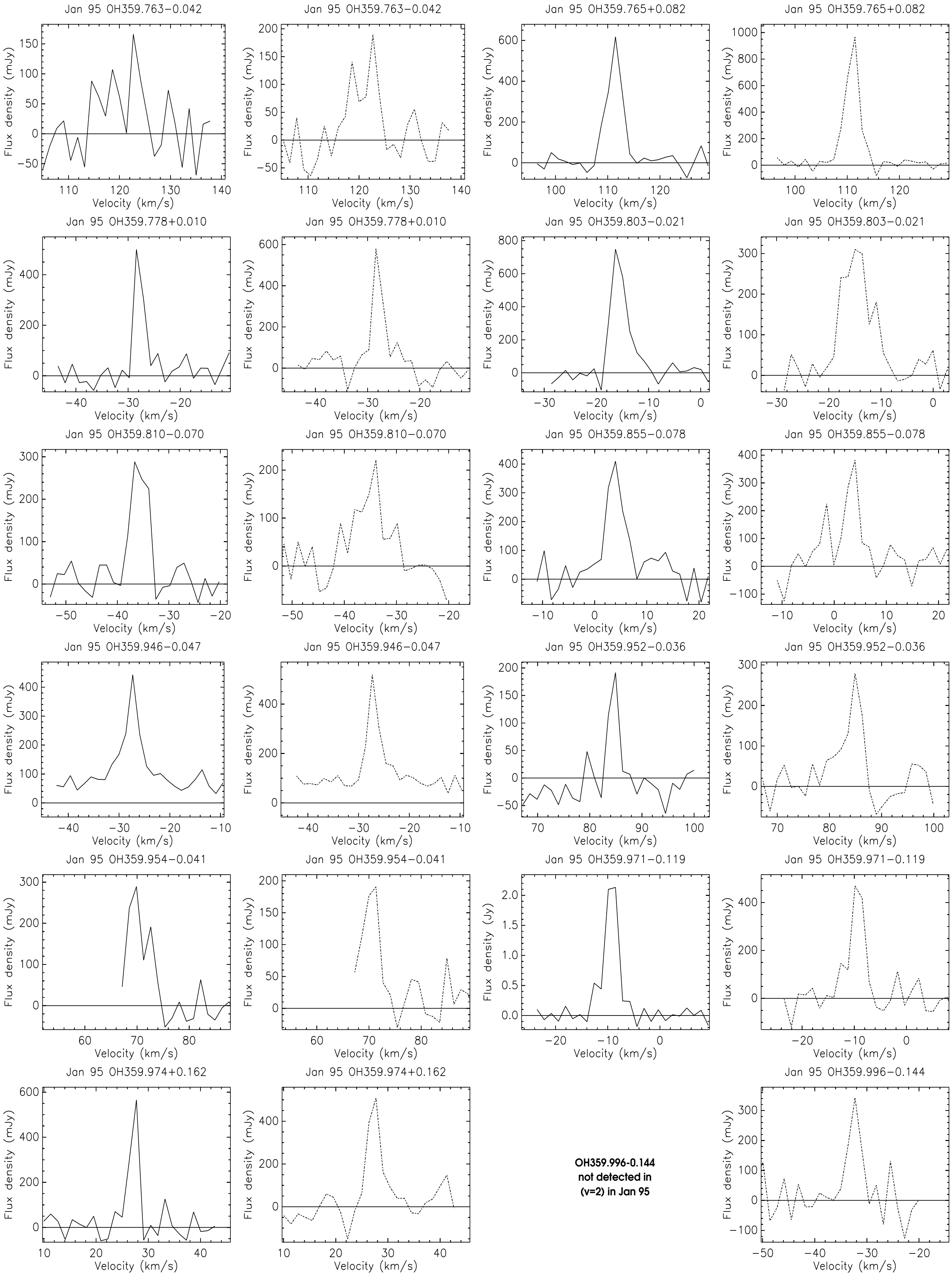


**Fig. 4.** Spectra of the 43 GHz SiO (J = 1 → 0) maser detections in January 1995. Solid lines (1st and 3rd column) are the spectra for ($v = 2$), the corresponding spectra for the ($v = 1$) lines are dotted on their right hand side (2nd and 4th column)

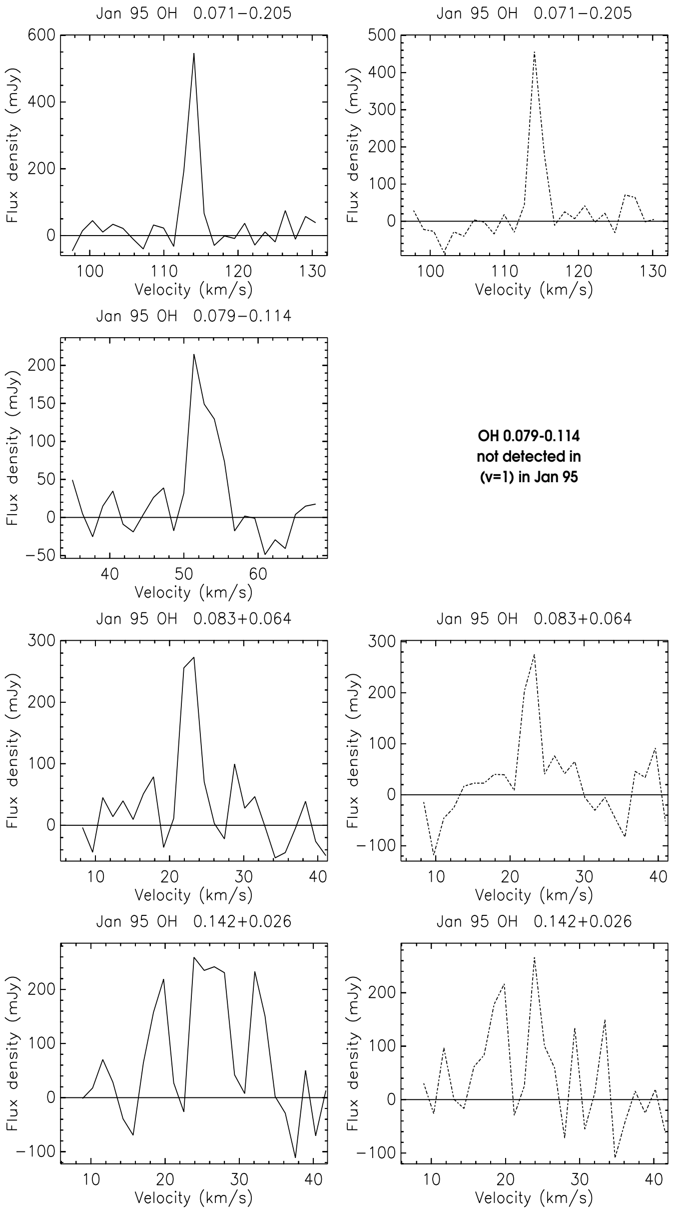


**Fig. 4.** 43 GHz SiO maser detections in January 1995; ($v = 2$) on the left hand side, ($v = 1$) on the right hand side (continued)

ble that the initial OH position in the catalog is not very accurate, because the Habing et al. (1983) observations were taken in the early days of the VLA. Sjouwerman et al. (1998b) concluded this source is probably not an OH/IR star, because the source has never been confirmed in the 1612 MHz OH line. However, with this $H_2O$ maser detection that matches the velocity of the detection in OH by Habing et al. (1983), and with a line-of-sight velocity of $\approx -130$ km s$^{-1}$, this object is probably of stellar origin.

**OH359.924−0.034:** Tentative association because of an offset to the OH position of slightly more than $5''$, and because the velocity is just below 100 km s$^{-1}$.

**OH359.936−0.144:** Seen as a single OH peak or possibly as double or triple 1612 MHz peak by Sjouwerman et al. (1998b), and because it resembles the $H_2O$ maser detection of OH359.751−0.371 we believe also this source has a young stellar origin. Similarly, this source has not been found as a compact continuum source because it is located at the edge of the Downes et al. (1979) survey.

**OH359.943+0.260:** Association based on the high velocity of the maser.

**OH359.946−0.047:** Clearly variable in the $H_2O$ maser, because it was not detected in July 93 (with good calibration available because it is in the beam of Sgr A*). Also detected as an $H_2O$ maser by Lindqvist et al. (1990). Publications by a group led by Menten seem not consistent about the observations of this source. In Menten & Reid (1998) the authors indicate to have found $H_2O$ emission from this source by the symbol used in their Fig. 1, but in Menten et al. (1997) the $H_2O$ maser is not mentioned. Also found as SiO maser by others (see references in Table 6).

**OH359.956−0.050:** OH name and OH position taken from Sjouwerman & van Langevelde (1996). This source was serendipitously found to be an $H_2O$ maser in a single pointing that targeted 5 known OH masers from the survey of Lindqvist et al. (1992). Also found as an $H_2O$ maser by Levine et al. (1995) and Yusef-Zadeh & Mehringer (1995), and as an SiO maser by Izumiura et al. (1998). It is one of the newly found OH/IR stars (Sjouwerman et al. 1998b) and its AGB nature is already extensively discussed in Sjouwerman & van Langevelde (1996) and e.g. Blum et al. (1996).

**OH 0.060−0.018:** It is the only $H_2O$ maser (except OH359.897−0.065, see above) in the high resolution VLA A-array (set 2a) with more than $1\farcs25$ offset from the OH maser. Its spectrum resembles a type A/B maser, but the offset from the OH maser is large and this tentative association is possibly with an SFR.

**OH 0.071−0.205:** A bit more offset than $5''$ from the targeted OH position, but within $5''$ of the position found for the SiO maser found here. Because of its high line-of-sight velocity, we associate this $H_2O$ maser with the OH maser.

**OH 0.134−0.023:** Tentative association because it is a bit further away ($6\farcs3$) from the OH maser than our criteria require for a positive association.

**OH 0.142+0.026:** At an offset of about $14''$ to the OH position, it is hard to argue for a type A/B $H_2O$ maser. The velocity coincidence is nevertheless striking, and the association therefore remains tentative.

**OH 0.178−0.055:** Spectrum exactly what one would expect for a type B $H_2O$ maser, but at large offset from the OH maser, and thus a tentative association.

**OH 0.190+0.0.036:** Tentative association; a high velocity source, but with an offset from the OH position larger than $8''$.

**OH 0.349+0.053:** Tentative association. An $H_2O$ maser source in the field toward the 1612 MHz OH maser source and close to the $H_2O$ and 1665/1667 MHz main-line OH maser $H_2O$/OH 0.37+0.04, observed with a single dish (Parkes) by Caswell et al. (1983), and Caswell & Haynes (1983) respectively. The latter do not report 1612 MHz OH maser emission for $H_2O$/OH 0.37+0.04.

However, their detection limit might have been too high. Apart from the position difference, all maser line detections are consistent with an OH/IR star as listed by Lindqvist et al. (1992).

**OH 0.543−0.043:** Found as a multiple peaked $H_2O$ and 1665 MHz OH maser by Mehringer et al. (1993), who classified it as one of the many SFR's in Sgr B1. However, the combination of the double peaked 1612 MHz and 1665 MHz maser emission and both their and our $H_2O$ maser profile point toward a Type I OH/IR star, resolving the issue in favor of the view of Lindqvist et al. (1992).

**OH 0.548−0.059:** Extrapolated visibility phases. Not seen in the $H_2O$ maser line by Mehringer et al. (1993) with good sensitivity, but observed in the 43 GHz SiO maser lines by Shiki et al. (1997). Because of its strong 43 GHz emission and large OH expansion velocity, they suggest that this is a foreground supergiant. Although the source therefore is probably less useful for the proper motion study, it might be very useful for calibration purposes.

**OH 0.589−0.108:** A high velocity $H_2O$ maser that is probably associated with the OH maser, but because of the extrapolated visibility phases offset by almost 8″.

### *4.2. Notes on the SiO masers*

Of the 16 SiO maser detections in January 1995, 4 had previously been detected in May 1994, whereas 2 SiO maser detections in May 1994 remained undetected in January 1995 (Table 5, Sect. 5.2).

A large fraction of the tentative SiO maser detections (May 1994, Sect. 3.2) were confirmed with emission close to the systemic (stellar) velocity derived from the OH maser profile in January 1995. Striking counter examples are **OH359.977−0.087** and **OH 0.007−0.088**. We are however convinced that they were detected in May 1994 (Fig. 1) and that the derived SiO positions are reliable (better than 1″ within the OH position in May 1994). We note that the former (OH359.98−0.09, Lindqvist et al. 1991) has been detected at 43 GHz previously. We attribute these two non-redetections to the SiO maser variability, which, next to lacking an SiO maser, also may be the case for the two real non-detections.

Sources **OH359.996−0.144** and **OH 0.079−0.114** were only detected in one of the 43 GHz lines. For **OH359.946−0.047** we subtracted a baseline, due to the extended continuum radiation of the Sgr A mini-spiral, before measuring the peak flux and the integrated line flux. Source **OH359.954−0.041** was unintentionally detected in the beam of OH359.952−0.036. Despite the unusual spectra for **OH359.763−0.042** and **OH 0.142+0.026** (which we do not attribute to high noise in the maps; see for comparison some SiO maser spectra in Mira-type stars in Jewell et al. 1991), we conclude that all SiO maser detections originate from the targeted OH/IR stars.

**Table 5.** Non-detections & Non-redetections

| | |
|---|---|
| May 1994 $H_2O$ maser survey: | |
| OH359.803−0.021 | OH359.946−0.047[b] |
| OH359.810−0.070 | OH359.952−0.036 |
| OH359.855−0.078[a] | OH359.954−0.041 |
| OH359.880−0.087 | OH359.955−0.031 |
| OH359.902+0.061 | OH359.996−0.144 |
| OH359.939−0.052 | OH 0.053−0.062 |
| January 1995 SiO maser survey: | |
| OH359.873−0.209 | OH359.977−0.087[b] |
| OH359.970−0.049 | OH 0.007−0.088[b] |

*a*: detected in July 1993 *b*: detected in May 1994

## 5. Discussion

The high frequency masers found in this survey are useful for follow-up VLBI observations if one has a reasonable chance of detecting them with VLBI arrays; i.e. their positions are well enough determined for the small field of views inherent to VLBI observations (typical 1″), and the maser is strong and stable enough.

### *5.1. Positions*

In order to estimate the internal accuracy (i.e. repeatability) of the individual OH/IR star positions, we have compared the positions of the $H_2O$ and SiO masers resulting from this survey with the input catalog, i.e. OH positions from Lindqvist et al. (1992). In the case where Lindqvist et al. (1992) have observed an OH/IR star more than once, usually their positions agree within an arcsecond, occasionally two, and similarly with the positions of e.g. van Langevelde et al. (1993). The Sjouwerman et al. (1998b) OH positions are not of direct use as a starting point for VLBI observations because they are known to deviate from previous catalogs: multiple epochs were aligned with self-calibration, introducing systematic offsets compared to e.g. the Lindqvist et al. (1992) positions of 1.″6, 1.″8 and 4.″2 for their c, b, and a data sets (e.g. Glass et al. 2001; Sjouwerman et al. 1998b; R. Ortiz, pers. comm.). If not stated otherwise, we used the Lindqvist et al. (1992) position with the smallest formal position error, which usually is the one closest to any of the pointing centers and thus suffers the least from sky curvature (see below). Note that the intrinsic size for the $H_2O$ and SiO maser shells, whether they are OH/IR stars or the more massive, larger shell size supergiants, is much less than an arcsecond; for OH/IR stars located at the GC, the SiO shell diameters typically measure 1 mas, and $H_2O$ maser shells are typically a few mas. From astrometric point of view, the higher frequency SiO masers are preferred to measure the stellar positions because of the higher resolution for a given interferometric array, as well as the accuracy to determine the stellar position from the maser position.

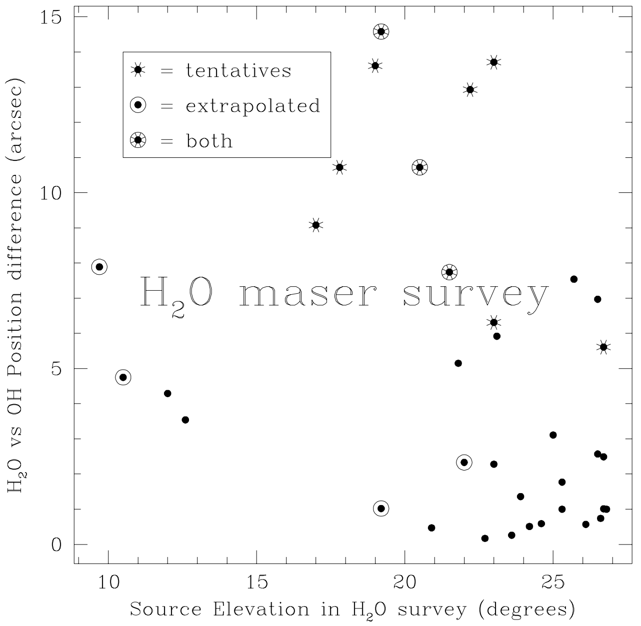


**Fig. 5.** $H_2O$ maser versus OH maser position difference versus source elevation at observation in the $H_2O$ survey. Starred symbols indicate tentative associations, circled symbols are detections made by extrapolating the visibility phases (i.e. the target scans are not two-sided enclosed by calibrator scans)

Excluding the 2 SFR's, for the $H_2O$ masers associated with the OH/IR stars we find that only 12, 11, and 7 of the positions agree with the original OH maser positions of (mainly) Lindqvist et al. (1992) within 2″, 1.″5, and 1″, respectively. If we assume that the positions coincide because they are close to the true position, and not due to chance alignment or the observing procedure used (see below), the OH and $H_2O$ maser positions only for these 7 to 12 stars thus can be considered to be relatively reasonably determined to the arcsecond level. Actually, a higher accuracy, preferably on sub-arcsecond level, is preferred if we were to use these positions as our starting points in detecting the masers with VLBI. Unfortunately, the quality of most $H_2O$ maser positions does not allow a statement of the internal accuracy of the maser positions.

In Sect. 4 we have reasoned that due to calibration problems, a difference of 5″ between the $H_2O$ and OH maser is acceptable for an association. Associations with larger deviations have been commented on in Sect. 4.1. This implies that at least these $H_2O$ maser positions may not be accurate enough for follow-up VLBI observations; the OH positions may be a better starting point. Although calibration errors are probably the main cause of differing positions, we have investigated whether any systematic biases are apparent. Lindqvist et al. (1992) have measured many tens of OH positions per field (with one field per observing day), whereas we continuously swap fields between our (assumed position of the) phase calibrator, Sgr A*, and our targets. Systematic effects could e.g. depend on distance to the field center due to neglecting 3-dimensional sky curvature in the imaging (for Lindqvist's OH masers), or position of, or distance to the phase calibrator (for the $H_2O$ and SiO masers in this survey). We have not found any systematic effects, even when we account for different observing runs. As the GC culminates at only 27° at the VLA, we show the $H_2O$ versus OH position differences as function of elevation at the time of observation in July 1993 or May 1994 in Fig. 5. We have introduced detections for positional differences of less than 5″, and tentative associations for positional differences of more than 8″. We are not surprised to see more tentative associations at the low end of the observed elevations at about 20°; possible tentative associations at the very low elevations probably already have been discarded by us in an earlier stage due to their larger offsets or phase calibration difficulties.

For the 18 SiO maser sources we find that 10, 15, and 17 of the positions coincide with the OH maser positions within 1″, 1.″5, and 2″, respectively. Only one SiO maser differs more, 2.″4 from the OH maser position, which might originate in the fact that the OH detection of Lindqvist et al. (1992) is weak in the second component, or because the SiO maser position for this source could be measured in the $(v = 1)$ line only (remarkably it is nevertheless within 1″ of the original position given by Winnberg et al. (1985), and about 1.″1 off from the Sjouwerman et al. (1998b) c-position). However, because in general the positions we measure in the $(v = 1)$ and $(v = 2)$ line are coincident on sub-arcsecond level, it is more likely that this relatively large difference between the OH and SiO maser position given for this source is in the fringe of measurement errors. Again, assuming that we are not comparing chance alignments, we conclude that the OH and SiO maser positions for these stars are relatively well determined to the arcsecond level.

Probably the best starting point for follow-up VLBI measurements, without reobserving the sample, is the average of the OH, $H_2O$ and/or SiO maser positions for the masers that independently coincide within 1-2″. Currently, with the OH maser positions of (mainly) Lindqvist et al. (1992) and the $H_2O$ and SiO masers of this work, we can make averages for 12 stellar $H_2O$ masers and 17 stellar SiO masers. Of those, 3 stars agree in positions in all three maser lines (OH359.855−0.078, OH359.946−0.047, and OH359.971−0.119).

### *5.2. Variability*

In contrast to the maser position, which can be improved by observations, the maser variability is of continuous concern for a VLBI campaign; one has to be able to find the source again after a few months or years. Fortunately for stellar objects, OH/IR and other AGB stars, the range in velocity of the maser emission is limited; for the SiO maser within ≈ 5 km/s from the systemic velocity. However, the maser flux varies considerably, in particular for the non-saturated $H_2O$ maser. A first impression of variability can be derived by collecting detections and non-detections

**Table 6.** Multiple and previous detections in OH/IR stars

| Name[a] | Previous/Other | | This work[d] | |
|---|---|---|---|---|
| OH | $H_2O$[b] | SiO[c] | $H_2O$ | SiO |
| 359.675+0.069 | + | + | | |
| 359.678−0.024 | − | + | | |
| 359.762+0.120 | | +,+[1] | | |
| 359.765+0.082 | | | + | + |
| 359.825−0.024 | − | + | | |
| 359.855−0.078 | | | +,− | + |
| 359.899+0.222 | − | + | | |
| 359.931−0.063 | | −,+[2] | | |
| 359.946−0.047 | +,±[3] | +[2,3,4,5] | −,+ | +,+ |
| 359.954−0.041 | + | +,+[2,4,5] | − | + |
| 359.956−0.050[d] | +[6,7] | +[2,4,5] | +,+ | |
| 359.970−0.049 | +[7] | +[5] | − | |
| 359.971−0.119 | − | + | + | + |
| 359.974+0.161 | | | | +,+ |
| 359.977−0.087 | − | + | | +,− |
| 359.986−0.061 | −,+[7] | + | | |
| 0.007−0.088 | | | | +,− |
| 0.040−0.056 | −,+[*] | + | + | |
| 0.071−0.205 | − | + | + | +,+ |
| 0.076+0.146 | + | − | + | |
| 0.083+0.064 | | | | +,+ |
| 0.113−0.060 | − | + | | |
| 0.142+0.026 | − | − | *t* | + |
| 0.189+0.052 | − | + | | |
| 0.543−0.043 | +[8] | | + | |
| 0.548−0.059 | −[8] | +[9] | + | |

*a*: Lindqvist et al. (1992)
*b*: Lindqvist et al. (1990)
*c*: Lindqvist et al. (1991)
*d*: See Tables 2, 4 and 5

±: See note in Sect. 4.1
∗: E. Schulman, pers. comm.
*t*: Tentative association

1: van Paradijs et al. (1995)
2: Miyazaki et al. (2001)
3: Menten et al. (1997)
4: Izumiura et al. (1998)
5: Deguchi et al. (2002)
6: Levine et al. (1995)
7: Yusef-Zadeh & M. (1995)
8: Mehringer et al. (1993)
9: Shiki et al. (1997)

from previous studies. We have made such an attempt, summarized in Table 6.

A simple count in Table 6 allows us to make a statement about the preferred maser taking into account the maser variability. Of the $H_2O$ masers observed more than once, only about one third is redetected. For the SiO masers, the redetection rate is much higher: 75%. Note that the *re*-detection rate is not dependent on the perhaps subjective selection of the sources (Sect. 3.2), as much of the data is from other observers. Of course this analysis is biased because no correction is made for sensitivity and never reported (mainly non-)detections, but it shows that variability is less of a problem for redetecting a given source in the 43 GHz SiO maser line. For measuring the proper motion on these variable OH/IR stars, the SiO maser also preferred above the less predictable $H_2O$ maser.

## 6. Conclusions

After excluding two $H_2O$ masers associated with SFR's, for initiating a VLBI campaign we have *stellar* positions consistent *within 1″* between the OH positions of Lindqvist et al. (1992) and this survey for 2 $H_2O$ masers, 7 SiO masers, and 3 stellar objects with both $H_2O$ and SiO masers (as well as the OH maser). They will be the best candidates for a proper motion campaign, without the need to find better initial positions. By averaging positions of the different masers that coincide within 1-2″ one may double the number of good starting positions for follow-up VLBI observations. The 43 GHz SiO masers are preferred over the 22 GHz $H_2O$ masers, not only because of the higher angular resolution at which positions can be determined, but also because the SiO maser is more easy to redetect than the $H_2O$ maser. Considering the variability of the sources, this number may be small for statistical analysis, but obtaining several proper motions might provide important information on the *type* of stellar orbits in the GC.

The total number of stellar high frequency masers, thus proper motion candidates, from this survey (excluding tentative associations) is 37: 25 $H_2O$, and 18 SiO, of which 6 detected in both maser lines. Of the 9 previously reported $H_2O$ masers in OH/IR stars, we observed 7 sources and confirmed 5. We observed 5 of the 17 previously reported SiO masers and confirm all 5. Combined with previous surveys, this totals to about 50 sources (see also references in Table 6). The current maser positions for the latter of these masers may not be accurate enough to detect them instantaneously with VLBI and thus need further astrometric observations.

The masers presented in this paper can be used to measure proper motions in the Galactic center, for example with the new Japanese VERA network, in order to determine the type of orbits and probe the Galactic center gravitational potential.

Serendipitously we have found 8 individual $H_2O$ masers in the molecular cloud M−0.13−0.08 and confirm that the masers found previously by Guesten & Downes (1983) and Okumura et al. (1989) are different masers.

*Acknowledgements.* In this paper we used observations obtained with the Very Large Array (VLA) of the National Radio Astronomy Observatory (NRAO). NRAO is operated by Associated Universities Inc. under cooperative agreement with the National Science Foundation. For data reduction facilities LOS acknowledges the hospitality of NRAO's Array Operations Center. LOS also acknowledges support for this research by the European Commission under contracts ERBFGECT 950012 and HPRI-CT-1999-00045. The authors also wish to thank the referee, D. Engels, for many helpful suggestions.

## References

Blitz, L., Binney, J., Lo, K. Y., Bally, J., & Ho, P. T. P. 1993, Nature, 361, 417

Blum, R. D., Sellgren, K., & Depoy, D. L. 1996, AJ, 112, 1988+
Bower, G. C., Backer, D. C., Wright, M., et al. 1997, ApJ, 484, 118+
Brand, J., Cesaroni, R., Caselli, P., et al. 1994, A&AS, 103, 541
Caswell, J. L., Batchelor, R. A., Forster, J. R., & Wellington, K. J. 1983, Australian Journal of Physics, 36, 401
Caswell, J. L. & Haynes, R. F. 1983, Australian Journal of Physics, 36, 361
Comoretto, G., Palagi, F., Cesaroni, R., et al. 1990, A&AS, 84, 179
Deguchi, S., Fujii, T., Miyoshi, M., & Nakashima, J. 2002, PASJ, 54, 61
Downes, D., Goss, W. M., Schwarz, U. J., & Wouterloot, J. G. A. 1979, A&AS, 35, 1
Engels, D. & Lewis, B. M. 1996, A&AS, 116, 117
Engels, D., Schmid-Burgk, J., & Walmsley, C. M. 1986, A&A, 167, 129
—. 1988, A&A, 191, 283
Engels, D., Winnberg, A., Walmsley, C. M., & Brand, J. 1997, A&A, 322, 291
Felli, M., Palagi, F., & Tofani, G. 1992, A&A, 255, 293
Frail, D. A., Diamond, P. J., Cordes, J. M., & van Langevelde, H. J. 1994, ApJ, 427, L43
Genzel, R. & Downes, D. 1977, A&AS, 30, 145
—. 1979, A&A, 72, 234
Genzel, R., Hollenbach, D., & Townes, C. H. 1994, Reports of Progress in Physics, 57, 417
Glass, I. S., Matsumoto, S., Carter, B. S., & Sekiguchi, K. 2001, MNRAS, 321, 77
Guesten, R. & Downes, D. 1983, A&A, 117, 343
Habing, H. J. 1996, A&A Rev., 7, 97
Habing, H. J., Olnon, F. M., Winnberg, A., Matthews, H. E., & Baud, B. 1983, A&A, 128, 230
Hachisuka, K. 2000, in EVN Symposium 2000, Proceedings of the 5th european VLBI Network Symposium held at Chalmers University of Technology, Gothenburg, Sweden, June 29 - July 1, 2000, Eds.: J.E. Conway, A.G. Polatidis, R.S. Booth and Y.M. Pihlström, published Onsala Space Observatory, p. 231, 231+
Honma, M., Oyama, T., Hachisuka, K., et al. 2000, PASJ, 52, 631
Iben, I. J. 1991, ApJS, 76, 55
Imai, H., Deguchi, S., Fujii, T., et al. 2002, PASJ, 54, L19
Izumiura, H., Deguchi, S., & Fujii, T. 1998, ApJ, 494, L89
Jewell, P. R., Snyder, L. E., Walmsley, C. M., Wilson, T. L., & Gensheimer, P. D. 1991, A&A, 242, 211
Levine, D. A., Figer, D. F., Morris, M., & McLean, I. S. 1995, ApJ, 447, L101
Lindqvist, M., Winnberg, A., & Forster, J. R. 1990, A&A, 229, 165
Lindqvist, M., Winnberg, A., Habing, H. J., & Matthews, H. E. 1992, A&AS, 92, 43
Lindqvist, M., Winnberg, A., Johansson, L. E. B., & Ukita, N. 1991, A&A, 250, 431
Mehringer, D. M., Palmer, P., & Goss, W. M. 1993, ApJ, 402, L69
Menten, K. M. & Reid, M. J. 1998, in ASP Conf. Ser. 144: IAU Colloq. 164: Radio Emission from Galactic and Extragalactic Compact Sources, 229+
Menten, K. M., Reid, M. J., Eckart, A., & Genzel, R. 1997, ApJ, 475, L111
Mezger, P. G., Duschl, W. J., & Zylka, R. 1996, A&A Rev., 7, 289
Miyazaki, A., Deguchi, S., Tsuboi, M., Kasuga, T., & Takano, S. 2001, PASJ, 53, 501
Morris, M. & Serabyn, E. 1996, ARA&A, 34, 645
Nyman, L.-A., Hall, P. J., & Le Bertre, T. 1993, A&A, 280, 551
Nyman, L.-A., Johansson, L. E. B., & Booth, R. S. 1986, A&A, 160, 352
Okumura, S. K., Ishiguro, M., Fomalont, E. B., et al. 1989, ApJ, 347, 240
Olnon, F. M., Winnberg, A., Matthews, H. E., & Schultz, G. V. 1980, A&AS, 42, 119
Reid, M. J. 1993, ARA&A, 31, 345
Reid, M. J., Schneps, M. H., Moran, J. M., et al. 1988, ApJ, 330, 809
Shiki, S., Ohishi, M., & Deguchi, S. 1997, ApJ, 478, 206+
Sjouwerman, L. O. & van Langevelde, H. J. 1996, ApJ, 461, L41
Sjouwerman, L. O., van Langevelde, H. J., & Diamond, P. J. 1998a, A&A, 339, 897
Sjouwerman, L. O., van Langevelde, H. J., Winnberg, A., & Habing, H. J. 1998b, A&AS, 128, 35
Te Lintel Hekkert, P., Versteege-Hensel, H. A., Habing, H. J., & Wiertz, M. 1989, A&AS, 78, 399
van Langevelde, H. J., Brown, A. G. A., Lindqvist, M., Habing, H. J., & de Zeeuw, P. T. 1992a, A&A, 261, L17
van Langevelde, H. J., Frail, D. A., Cordes, J. M., & Diamond, P. J. 1992b, ApJ, 396, 686
van Langevelde, H. J., Janssens, A. M., Goss, W. M., Habing, H. J., & Winnberg, A. 1993, A&AS, 101, 109+
van Paradijs, J., Spruit, H. C., van Langevelde, H. J., & Waters, L. B. F. M. 1995, A&A, 303, L25
Winnberg, A., Baud, B., Matthews, H. E., Habing, H. J., & Olnon, F. M. 1985, ApJ, 291, L45
Yusef-Zadeh, F. & Mehringer, D. M. 1995, ApJ, 452, L37